RAPID COMMUNICATIONS

PHYSICAL REVIEW B VOLUME 36, NUMBER 5 15 AUGUST 1987-I

Momentum-mixing-induced enhancement of band nonparabolicity in GaAs-$Ga_{1-x}Al_xAs$ superlattices

L. D. L. Brown, M. Jaros, and D. Ninno
Department of Theoretical Physics, The University, Newcastle upon Tyne, NEI 7RU United Kingdom

(Received 2 February 1987; revised manuscript received 4 May 1987)

We report a pseudopotential calculation of the conduction-band nonparabolicity in GaAs-$Ga_{1-x}Al_xAs$ superlattices of period ~80 Å. We find that even in structures with a significant energy separation between the lowest Γ- and X-related subbands the lowest-subband nonparabolicity is enhanced as a result of virtual excitations to higher states of mixed-momentum character.

There has been considerable interest in the relationship between miniband nonparabolicity and microstructure parameters (e.g., well widths and material composition) of semiconductor superlattices.[1,2] For example, the electron velocity in a symmetric nonparabolic band is a cubic function of momentum and the system exhibits interesting nonlinear properties.[3-5] It is well known from band theory that the band curvature is linked to the structure of the higher-lying bands. For example, the effective mass is proportional to the second derivative, d^2E/dk^2, of the band energy with respect to wave vector. The effective mass can be rigorously expressed as a second-order $\mathbf{k}\cdot\mathbf{p}$ perturbation expansion. This expansion involves momentum matrix elements between a given band and all other bands. Similarly, the fourth derivative, d^4E/dk^4, can be evaluated from a fourth-order $\mathbf{k}\cdot\mathbf{p}$ perturbation expansion.[6] It has been shown[7] that the effective mass of the lowest conduction state is significantly increased due to virtual transitions to states of mixed character, i.e., states containing contributions from both the bulk Γ and X minima. Similarly, it follows that in a superlattice the lowest-miniband nonparabolicity must be significantly affected by the properties of the higher subbands. The character of these higher bands cannot be accurately described by approximate methods and their effect so far has largely been ignored. We have recently carried out pseudopotential calculations of the electronic structure of semiconductor superlattices in which the higher-lying bands are well accounted for. In this study, we evaluate the lowest-conduction-subband nonparabolicity in GaAs-$Ga_{1-x}Al_xAs$ superlattices. We show for the first time that in certain commonly known structures the resonances derived from the primary Γ minima, together with the states associated with the X minimum, play a key role in determining the nonparabolicity of the lowest conduction subband. This effect occurs independently of, and in addition to, other smaller corrections due to the nonparbolicity of the bulk Γ valley (which can to some extent be incorporated into the effective-mass approximation).

We use relativistic pseudopotentials to generate the superlattice band structure, energies, and wave functions. Starting with a suitable semiempirical Hamiltonian to represent GaAs in the relevant range of energies, the bulk band energies $E_{n,\mathbf{k},s}$, and wave functions $\phi_{n,\mathbf{k},s}$, are obtained in good agreement with experiment. The superlattice wave function ψ is constructed as a linear combination of $\phi_{n,\mathbf{k},s}$,

$$\psi=\sum_{n,\mathbf{k},s} A_{n,\mathbf{k},s}\phi_{n,\mathbf{k},s} \ , \tag{1}$$

where n is the band index, $\mathbf{k}$ the wave vector, and s is the spin variable. The Schrödinger equation is solved by direct diagonalization. The technical details concerning our method of calculation are described in detail elsewhere.[7] We have shown that our calculations can account for energy levels and oscillator strengths in quantum-well structures with a meV accuracy.[8] To obtain an accurate value of d^4E/dk^4 for the lowest conduction subband at the band minimum from our pseudopotential band structure, Kane's $\mathbf{k}\cdot\mathbf{p}$ perturbation theory is employed. At $\mathbf{k}=\mathbf{0}$ the expression for d^4E/dk^4 reduces to

$$\left.\frac{d^4E}{dk^4}\right|_{k=0}=+\sum_{\substack{m(\neq n)\\ q(\neq n)\\ r(\neq n)}}\left(-\frac{M_{nm}M_{rn}M_{qr}M_{mq}}{E_{mn}E_{qn}E_{rn}}+\frac{M_{nr}M_{mr}M_{rn}}{E_{mn}E_{rn}^2}+\frac{M_{nn}M_{nm}M_{rn}M_{mr}}{E_{mn}^2E_{rn}}+\frac{|M_{nr}|^2|M_{mn}|^2}{E_{mn}^2E_{rn}}-\frac{|M_{nn}|^2|M_{mn}|^2}{E_{mn}^3}\right), \tag{2}$$

where m,n,q,r are band indices, n is the superlattice miniband for which the derivative is found, and $E_{ab}=E_a-E_b$. M_{ab} is an optical matrix element which in the usual electric dipole approximation reduces to

$$M_{ab}=\langle\psi_a|\epsilon\cdot(-i\nabla)|\psi_b\rangle \ . \tag{3}$$

The direction of the polarization vector ϵ is along the superlattice axis ⟨001⟩. In our calculation, all terms in (2) which contribute to d^4E/dk^4 are included.

To help visualize the virtual excitations in (2), the positions of the confined states of Γ and X character in a GaAs-$Ga_{0.7}Al_{0.3}As$ superlattice (56-Å wells and 22-Å barriers, $x=0.3$), obtained at the zone center ($\mathbf{k}=\mathbf{0}$), are shown in Fig. 1. One of the "allowed" four-stage excita-

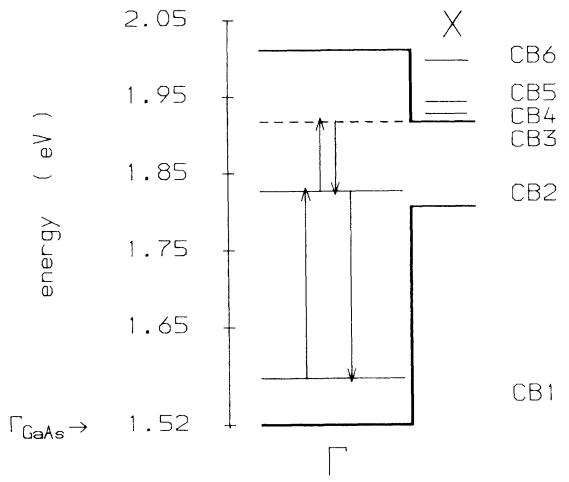

FIG. 1. The Γ-X well alignment for the GaAS (56 Å)-$Ga_{0.7}Al_{0.3}As$ (22 Å) superlattice together with the lowest-lying states obtained at $\mathbf{k}=\mathbf{0}$. A possible four-stage virtual excitation process is shown schematically. Only states at the conduction-band edge are shown.

tion processes of (2) is indicated by arrows. The band structure of this superlattice near the conduction-band (CB) edge is shown in Fig. 2, across the full length of the superlattice Brillouin zone along ⟨001⟩. We can see there explicitly the shape and position of the six lowest subbands labeled CB1-CB6. We are interested in the role of mixing of the bulk momentum Γ and X components,

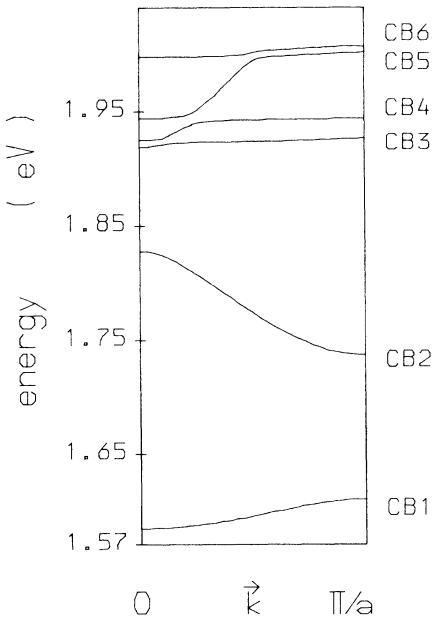

FIG. 2. The miniband structure for a GaAs (56 Å)-$Ga_{0.7}Al_{0.3}As$ (22 Å) superlattice across the minizone, along ⟨001⟩ direction. The dispersion of the six lowest conduction minibands (see Fig. 1) is shown.

which gives a qualitative meaning to the value of matrix elements between superlattice wave functions. It is, therefore, instructive to inspect Fig. 3 where we plot the corresponding superlattice-wave-function coefficients $|A_{n,\mathbf{k},s}|^2$. This figure shows that the wave functions of the lowest two conduction minibands are built from bulk wave functions clustered around the bulk Γ minimum. However, the higher subbands (CB3-CB6) contain significant contributions from bulk X wave functions. The mixing of bulk wave functions is most apparent in state CB3. It is caused by folding of the bulk bands and enhanced by the effect of the short-wavelength components of the superlattice potential.[9]

When the alloy composition x is changed, the separation of the levels shown in Fig. 1 change. Increasing x from $x=0$ increases the height of the confining barrier (i.e., the separation between the conduction-band edges of GaAs and $Ga_{1-x}Al_xAs$). The state CB3 which lies just above the barrier is being pushed towards the lowest X miniband as x increases. The lowest X miniband lies at the bulk X point of the barrier material, and the Γ-X mixing in the wave function of state CB3 increases. Since the X-point Bloch states contain a p-like momentum contribution, the matrix element between, say, the s-like state CB2 and CB3 increases. Near $x\sim 0.35$, where states CB3 and CB4 cross, the fourth derivative (2) has a maximum. At this point d^4E/dk^4 is about six times larger than in

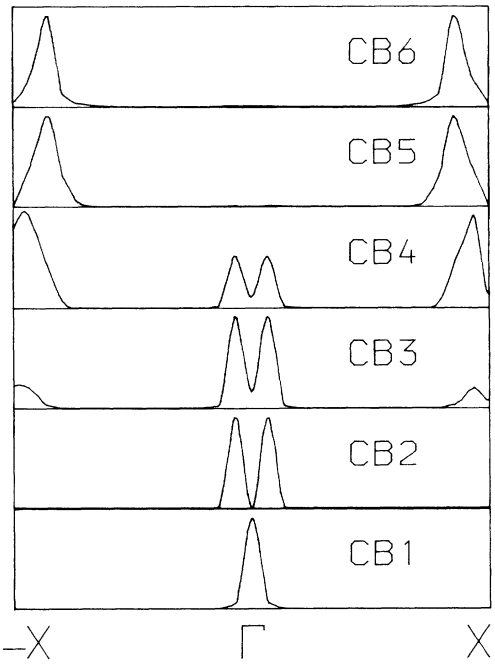

FIG. 3. Plot of the sum over the spin of the modulus squared of the wave-function coefficients $|A_{n,\mathbf{k},s}|^2$ for the states in Fig. 1, demonstrating the momentum mixing in the higher-lying conduction states. The $|A_{n,\mathbf{k},s}|^2$ are scaled in such a way that the largest term is set equal to one. Only contributions associated with the lowest bulk conduction band of bulk GaAs in expansion (1) are shown. Γ and X refer to the bulk Brillouin zone of GaAs.

bulk GaAs.

Increasing the barrier height also tends to reduce the leakage of the wave function of states CB1 and CB2 into the barrier and consequently reduces the overlap with state CB3 which is mainly localized in the barrier.[9] This mechanism acts against the enhancement referred to above and contributes to a reduction of band nonparabolicity. The results of our full calculation which reflect these two trends very clearly are shown in Fig. 4 (upper curve). The transitions in (2) from the first conduction state to the valence band involve energy denominators which are typically an order of magnitude greater than the energy separations between neighboring conduction states. Consequently, the effect of the valence states is small.

Our result in Fig. 4 is in sharp contrast with that predicted by simple models. For example, the lower curve shown in Fig. 4 was obtained by the method of Cooperman, Friedman, and Bloss[5] based on the Kronig-Penney model. It shows decreasing d^4E/dk^4 with decreasing x. This is not surprising since for fixed well and barrier width and fixed well material (GaAs) the only compositionally dependent parameter becomes the barrier height. In particular, the multivalley character of the conduction band is not taken into account.

Mobile electrons in a symmetric nonparabolic band have a nonlinear velocity-momentum relation. An external electromagnetic field applied to such a system causes the electron momentum to follow the frequency of the applied field. The nonlinear velocity component causes the induced current to contain mixed frequency components.[3,4] The magnitude of this nonlinearity is measured by the third-order nonlinear susceptibility $\chi^{(3)}$, which is proportional to the fourth derivative of the band energy versus wave vector.[5]

The bulk-conduction-band nonparabolicity in GaAs is quite small.[4] However, we have seen that a significant enhancement of d^4E/dk^4 and consequently of $\chi^{(3)}$ can be achieved in superlattices by a suitable choice of well widths and barrier heights (and consequently secondary band-edge alignment). Our results presented in Fig. 4 show that the momentum mixing which reflects the multivalley character of the conduction band of $Ga_{1-x}Al_xAs$ cannot be ignored. In a superlattice, this mixing alters the character of higher-lying states which can , owing to the effects of zone folding, make significant contributions to the virtual excitations on which d^4E/dk^4 depends. In particular, the results presented in this study show that even in structures where the lowest Γ-related subband lies well below the X-like states, the curvature of this subband may depend on the position and localization of the X-like subbands. In the example chosen here the zone-folding induced momentum mixing enhances d^4E/dk^4 by six times that of bulk GaAs. It follows that even if the energy levels lying deep in the confining wells can be accounted for by a simple model (e.g., a modified effective mass like Hamiltonian or "Kronig-Penney-like" models) the nonlinear properties of the system are *not* well represented and must be carefully assessed in terms of a full scale calculation.

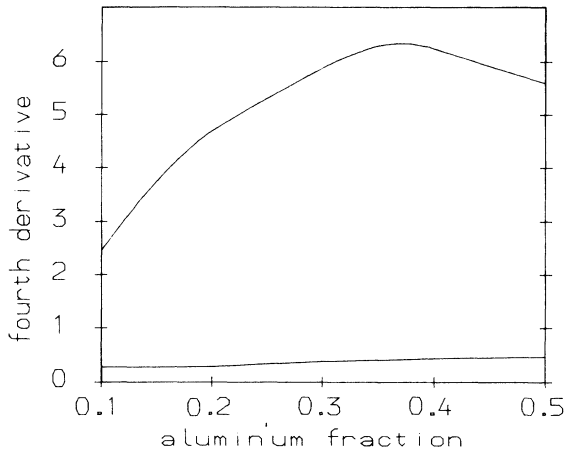

FIG. 4. The ratio of the fourth derivative of the lowest conduction state in a GaAs (56 Å)–$Ga_{1-x}Al_xAs$ (22 Å) superlattice to that of bulk GaAs, as a function of aluminum fraction. The upper curve refers to a fully convergent pseudopotential calculation at $\mathbf{k}=\mathbf{0}$ [see Eq. (2)]. The lower curve is based on the Kronig-Penney model with the same parameters. Note that our curve exhibits a distinct peak near $x\sim 0.35$ at which the Γ resonance CB3 crosses the lowest X-related subband CB4. The interaction accounts for the dominant contribution in Eq. (2).

We wish to thank the Science and Engineering Research Council (United Kingdom) for financial support.

[1]R. C. Miller, C. W. Tu, S. K. Sputz, and R. F. Kopf, Appl. Phys. Lett. **49**, 1245 (1986).

[2]T. Hiroshima and R. Lang, Appl. Phys. Lett. **49**, 456 (1986).

[3]P. A. Wolff and G. A. Pearson, Phys. Rev. Lett. **17**, 1015 (1966).

[4]C. K. N. Patel, R. E. Slusher, and P. A. Fleury, Phys. Rev. Lett. **17**, 1011 (1966).

[5]G. Cooperman, L. Friedman, and W. L. Bloss, Appl. Phys. Lett. **44**, 977 (1984).

[6]E. O. Kane, J. Phys. Chem. Solids **1**, 259 (1957).

[7]M. A. Gell, D. Ninno, M. Jaros, and D. C. Herbert, Phys. Rev. B **34**, 2416 (1986); M. A. Gell, D. Ninno, M. Jaros, D. J. Wolford, T. F. Keuch, and J. A. Bradley, *ibid.* **35**, 1196 (1987).

[8]D. Ninno, M. A. Gell, and M. Jaros, J. Phys. C **19**, 3845 (1986).

[9]D. Ninno, K. B. Wong, M. A. Gell, and M. Jaros, Phys. Rev. B **32**, 2700 (1985).